Downloaded from genesdev.cshlp.org on April 30, 2024 - Published by Cold Spring Harbor Laboratory Press

Ablation of the CDK inhibitor p57^{Kip2} results in increased apoptosis and delayed differentiation during mouse development

Yimin Yan,[1] Jonas Frisén,[1,4] Mong-Hong Lee,[2,3] Joan Massagué,[2] and Mariano Barbacid[1,5]

[1]Department of Molecular Oncology, Bristol-Myers Squibb Pharmaceutical Research Institute, Princeton, New Jersey 08543 USA; [2]Cell Biology and Genetics Program, Memorial Sloan-Kettering Cancer Center, Howard Hughes Medical Institute, New York, New York 10021 USA

$p57^{Kip2}$ is a paternally imprinted gene that encodes a potent inhibitor of several cyclin/Cdk complexes. p57^{Kip2} is primarily expressed in terminally differentiated cells, associates with G_1 Cdks, and can cause cell cycle arrest in G_1 phase. To investigate the role of p57^{Kip2} in vivo, we have ablated the $p57^{Kip2}$ gene by homologous recombination in ES cells and generated mice devoid of p57^{Kip2} expression. Most $p57^{Kip2}$ *null* mice die after birth and display severe developmental defects with varying degrees of penetrance. As expected, heterozygous mice that inherit a maternal, but not a paternal, targeted allele exhibit similar deficiencies and neonatal death. Developmental defects of $p57^{Kip2}$ mutant mice include cleft palate and gastrointestinal abnormalities ranging from an inflated GI tract to loss of the jejunum and ileum. These tissues display a significant increase of apoptotic cells in the absence of p57^{Kip2}. Most $p57^{Kip2}$ mutant mice have short limbs, a defect attributable to abnormal endochondral ossification caused by delayed cell cycle exit during chondrocyte differentiation. A similar defect has been observed in mice lacking p107 and p130, thus suggesting that p57^{Kip2} might be an upstream regulator of these Rb-related proteins. The $p57^{Kip2}$ locus has been implicated in the Beckwith–Wiedemann syndrome and in the development of sporadic Wilms' tumors and lung carcinomas. To date, we have not observed neoplastic development even in those $p57^{Kip2}$ mutant mice that have survived for >5 months of age. These findings indicate that p57^{Kip2} has an important role during mouse development that cannot be compensated by other Cdk inhibitors.

[*Key Words:* Cell cycle; cyclin-dependent kinase; apoptosis; differentiation; development]

Received February 6, 1997; revised version accepted March 14, 1997.

Cells become committed to divide when they meet the requirements for entry into S phase. When these requirements are not met, either because of insufficient mitogenic stimulation or prevalence of antimitogenic mechanisms, cells may progress from G_1 phase toward quiescence or terminal differentiation. These fates are determined, in part, by the activity of cyclin-dependent kinases (Cdks). The activity of Cdk2, Cdk4, and Cdk6 is essential for G_1 progression into S phase and is tightly controlled by both positive and negative regulators (Norbury and Nurse 1992; Hunter and Pines 1994). The function of these regulators is therefore critical for normal embryonic development as well as for maintenance of proper homeostasis in the adult organism.

Present addresses: [3]Department of Surgical Oncology and Tumor Biology, M.D. Anderson Cancer Center, University of Texas, Houston, Texas 77030 USA; [4]Department of Neuroscience, Karolinska Institute, S-17177 Stockholm, Sweden.
[5]Corresponding author.
E-MAIL barbacid@bms.com; FAX (609) 252-6051.

Over the past few years, proteins that function as stoichiometric inhibitors of G_1 Cdk have emerged as major regulators of Cdk activity (Sherr and Roberts 1995). These proteins may function as regulators of mammalian development, and their loss may cause hyperproliferative disorders. Two families of mammalian Cdk inhibitors have been identified. The Ink4 family includes four members, p16^{Ink4a}, p15^{Ink4b}, p18^{Ink4c}, and p19^{Ink4d}, which are specific inhibitors of Cdk4 and Cdk6 (Sherr and Roberts 1995). $p16^{Ink4a}$ is a tumor suppressor gene located in human chromosome 9p21 and deleted or mutated in hereditary melanomas and in several sporadic cancers (Hall and Peters 1996). $p16^{Ink4a}$ *null* mice have abnormal hematopoiesis and are highly susceptible to development of sarcomas and B-cell lymphomas (Serrano et al. 1996). These and other observations suggest that p16^{Ink4a} may normally function to limit the life span of the cell (Hall and Peters 1996). p15^{Ink4b}, on the other hand, is under positive control by transforming growth factor-β (TGF-β) (Hannon and Beach 1994; Reynisdóttir

Downloaded from genesdev.cshlp.org on April 30, 2024 - Published by Cold Spring Harbor Laboratory Press

et al. 1995), and its induction by this cytokine mediates G_1 arrest (Reynisdóttir and Massagué 1997). The *p15^{Ink4b}* locus maps on 9p21, almost next to *p16^{Ink4a}*. Deletions in this tumor suppressor gene often affect *p15^{Ink4b}* as well (Hall and Peters 1996). The functions of p18^{Ink4c} and p19^{Ink4d} are largely unknown (Sherr and Roberts 1995).

The Cip/Kip family of mammalian Cdk inhibitors includes three members, p21$^{Cip1/WAF1}$, p27^{Kip1}, and p57^{Kip2} (Sherr and Roberts 1995). Cip/Kip proteins inhibit G_1 cyclin–Cdk complexes by binding to the cyclin subunit and blocking the catalytic site of the associated Cdk subunit (Russo et al. 1996). p21$^{Cip1/WAF1}$ and p27^{Kip1} have been implicated as mediators of the antimitogenic action of diverse agonists. For example, p21$^{Cip1/WAF1}$ expression is elevated by a p53-dependent mechanism in response to DNA damage (El-Deiry et al. 1994). Increased levels of p21$^{Cip1/WAF1}$ cause Cdk inhibition and a delay in G_1 (Harper et al. 1993). p21$^{Cip1/WAF1}$ expression is also increased in response to TGFβ (Datto et al. 1995; Reynisdóttir et al. 1995), whereas the expression of p27^{Kip1} is increased upon mitogen withdrawal or contact inhibition (Kato et al. 1994; Nourse et al. 1994; Polyak et al. 1994; Slingerland et al. 1994; Toyoshima and Hunter 1994). p21$^{Cip1/WAF1}$ and p27^{Kip1} are elevated in response to differentiation agents in vitro (Steinman et al. 1994; Liu et al. 1996) and during cell differentiation in vivo (Havely et al. 1995; Parker et al. 1995; Lee et al. 1996). The physiological role of these Cdk inhibitors has been investigated recently by gene targeting in embryonic stem (ES) cells. *p21$^{Cip1/WAF1}$ null* mice do not show developmental defects or elevated tumor incidence. However, fibroblasts derived from these animals are partially deficient in radiation-induced G_1 arrest (Brugarolas et al. 1995; Deng et al. 1995). *p27^{Kip1}* null mice have increased size and cellularity in many adult organs and are predisposed to tumors of the pituitary (Fero et al. 1996; Kiyokawa et al. 1996; Nakayama et al. 1996). However, the lack of *p21$^{Cip1/WAF1}$* or *p27^{Kip1}* function does not lead to gross developmental defects, suggesting the existence of compensatory mechanisms during development. Interestingly, *dacapo*, a new member of the Cip/Kip family of Cdk inhibitors identified in *Drosophila*, has a key role during embryogenesis by regulating the timely exit of certain cells from the cell cycle (de Noolj et al. 1996; Lane et al. 1996).

Much less is known about the role of p57^{Kip2}. This inhibitor differs structurally from p21$^{Cip1/WAF1}$ and p27^{Kip1} in that it has a long insert consisting of proline/alanine-rich or acidic motifs following the conserved Cdk inhibitory domain (Lee et al. 1995; Matsuoka et al. 1995). Interest in p57^{Kip2} also arises from the fact that its gene maps to chromosome 11p15 (Matsuoka et al. 1995) and is paternally imprinted in mice and humans (Hatada and Mukai 1995; Matsuoka et al. 1996). These are properties predicted for a tumor suppressor gene linked to the Beckwith–Wiedemann syndrome, a genetic defect characterized by prenatal organ overgrowth and predisposition to embryonal tumors, including Wilms' tumor and rhabdomyosarcoma (Scrable et al. 1989). Misense and frameshift mutations in *p57^{Kip2}* have been identified recently in the maternal allele of two patients with Beckwith–Wiedemann syndrome (Hatada et al. 1996). *p57^{Kip2}* may also be involved in the development of somatic tumors. For instance, it has been reported recently that 11 of 13 lung carcinomas carrying 11p15 deletions have selectively lost their maternal allele (Kondo et al. 1996). Moreover, Wilms' tumors have drastically reduced levels of *p57^{Kip2}* transcripts (5%–10% of those found in matched normal kidney tissue from the same patients) (Thompson et al. 1996). These observations suggest that absence or decreased expression of p57^{Kip2} may have a role in the development of certain forms of human cancer.

To investigate the physiological role of p57^{Kip2}, we have generated mice carrying a targeted deletion in the *p57^{Kip2}* locus. *p57^{Kip2} null* mice have major developmental defects in the formation of palate, intestine, and endochondral bone, apparently resulting from increased apoptosis (palate and intestine) or proliferation at the expense of cell differentiation (endochondral bone). Thus, in contrast to the other mammalian Cdk inhibitors analyzed to date, p57^{Kip2} has an essential role as a cell cycle regulator during mouse development.

Results

Expression of p57^{Kip2} during embryogenesis

We have analyzed the expression of the cell cycle regulator p57^{Kip2} during embryonic development. To this end, we submitted frozen sections obtained from embryos at various stages of development to immunohistochemical analysis using a polyclonal antibody generated against a carboxy-terminal peptide from p57^{Kip2} (see Materials and Methods). At embryonic day 10.5 (E10.5), we observed high p57^{Kip2} immunoreactivity in newly differentiated neurons that have finished their last cell cycle and are in the process of migrating out of the ventricular zone (Fig. 1a). Little or no p57^{Kip2} expression could be found in the ventricular zone where progenitor cells are proliferating. High levels of p57^{Kip2} expression were also observed in the somites (Fig. 1a) and in muscle cells of the developing heart (Fig. 1b). No significant p57^{Kip2} immunoreactivity could be detected in other tissues at this developmental stage.

During mid- and late embryogenesis, p57^{Kip2} is expressed in additional tissues and structures, presumably as more cells exit the cell cycle and start the process of terminal differentiation. For instance, E17.5 embryos display significant levels of p57^{Kip2} immunoreactivity in various muscle cells, including those of cardiac (data not shown) and skeletal muscle (Fig. 1c). p57^{Kip2} is also highly expressed in epithelial cells during late embryogenesis. For instance, E17.5 embryos display high levels of p57^{Kip2} immunoreactivity in the differentiated epithelia of the renal glomeruli and some of the renal ducts (Fig. 1d) as well as in the epithelial cells of the lens (Fig. 1e). In the intestinal epithelia, p57^{Kip2} is expressed in the differentiated cells of the apical region of the villi but not

Downloaded from genesdev.cshlp.org on April 30, 2024 - Published by Cold Spring Harbor Laboratory Press

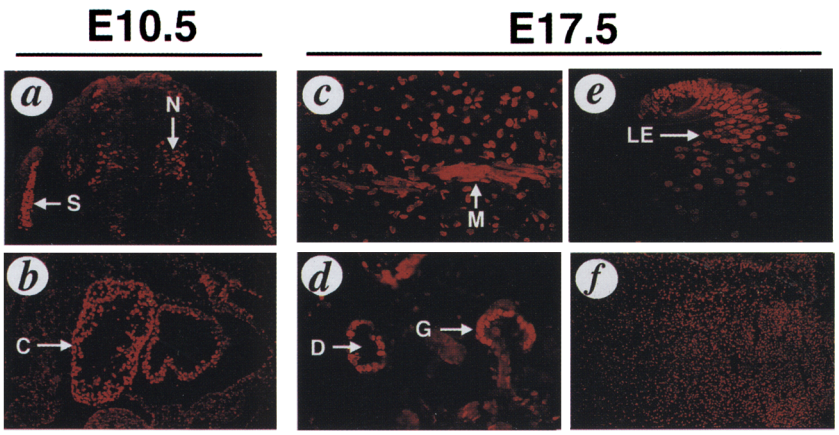

Figure 1. p57^{Kip2} expression during embryonic development. Frozen sections (10 μm thick) from E10.5 (*a*,*b*) and E17.5 (*c*–*f*) embryos were incubated with anti p57^{Kip2} antibodies. (*a*) Cross section of the neural tube. Newly generated neurons (N) migrate from the ventricular zone and are strongly labeled; somites (S) are also stained intensely. (*b*) High level of p57^{Kip2} expression in cardiac muscle (C). (*c*) Robust expression of p57^{Kip2} in skeletal muscle cells. (M) An elongated nucleus. (*d*) p57^{Kip2} expression in the kidney is localized in the differentiated epithelial cells of the glomeruli (G) and some of the ducts (D). (*e*) High levels of p57^{Kip2} expression in lens epithelial cells (LE). (*f*) Coronal section of palate displaying p57^{Kip2} expression in most cells.

in the dividing cells of the crypts (see below), suggesting that p57^{Kip2} may be up-regulated when cells exit the cell cycle and start their differentiation program. p57^{Kip2} is also highly expressed in the palate (Fig. 1f). In general, these observations are in agreement with previous studies using Northern blot analysis and in situ hybridization techniques (Lee et al. 1995; Matsuoka et al. 1995).

Targeted disruption of the p57^{Kip2} locus

Analysis of the genomic structure of the human *p57^{Kip2}* locus has revealed four exons of which only two (second and third) encompass coding sequences (Tokino et al. 1996). Analysis of genomic clones of 129/Sv mice revealed a similar organization (Fig. 2a). Whereas the 922-bp-long second exon contains those sequences encoding the start codon, the CDK inhibitory domain, the proline-rich domain, and the acidic domain, the third exon codes for the 44 carboxy-terminal amino acid residues (Lee et al. 1995; Matsuoka et al. 1995). To ablate the *p57^{Kip2}* gene, we designed a targeting plasmid, designated pYY2, which contains a phosphoglycerokinase (PGK)–*neo* cassette used for positive selection (see Materials and Methods) flanked by 4 kb (left arm) and 7.5 kb (right arm) of mouse 129/Sv genomic sequences (Fig. 2a). A PGK–thymidine kinase cassette used for negative selection was placed 3′ of the genomic sequences. Homologous recombination with this targeting plasmid results in the elimination of 1.1 kb of *p57^{Kip2}* genomic sequences that encompass the entire first exon and about half of the second exon, including those nucleotides encoding amino acid residues 1–181 of the p57^{Kip2} protein.

ES cells (R1 clone) were transfected with pYY2 DNA and incubated in the presence of G418 and gancyclovir (Klein et al. 1993). Double resistant colonies were expanded and submitted to Southern blot analysis to determine the occurrence of homologous recombination. Of 183 G418^{R}/Gan^{R} ES cell clones analyzed, two, clones B302-36 and B302-319, displayed the diagnostic DNA fragments (Fig. 2b). To generate chimeric mice containing the targeted *p57^{Kip2}* allele, these ES clones were either microinjected into C57BL/6 blastocysts or aggregated with cells derived from morulas of ICR mice. Male chimeras were bred to wild-type mice from the corresponding strain until the targeted *p57^{Kip2}* allele was transmitted to their offspring. C57BL/6 and ICR chimeras derived from clone B302-319 and ICR chimeras derived from B302-36 cells yielded germ-line transmission of the mutant *p57^{Kip2}* allele. The phenotypes of the *p57^{Kip2}* mutant mice (see below) generated from these ES cell clones were grossly the same. Moreover, no significant differences were observed when mutant mice derived from the B302-319 clone were maintained in a mixed 129/Sv–C57BL/6 or 129/Sv–ICR genetic background. Offspring derived from the B302-319 ES cell clone in a mixed 129/Sv–C57BL/6 genetic background were selected for detailed characterization in this study.

Early postnatal death of p57^{Kip2} *(−/−) mutant mice*

Genotypic analysis of 200 live births derived from matings between *p57^{Kip2}* heterozygous mice revealed that 56 (28.0%) were (+/+), 97 (48.5%) were (+/−), and 47 (23.5%) were (−/−). The slightly higher than expected percentage of wild-type animals suggests limited embryonic lethality of those embryos carrying the targeted allele. This was confirmed in subsequent breedings when we observed the presence of dead (+/−) and (−/−) embryos at stages ranging from E10.5 to E16.5. Moreover, about half of the (+/−) and most of the (−/−) newborn mice died within several hours after birth and displayed various anatomical defects. The presence of developmental defects in the heterozygous animals is most likely a consequence of paternal imprinting in this locus (Hatada and Mukai 1995) (see below).

Forty-one of the 47 (−/−) mice (87.2%) died at postnatal day 0/1 (P0/P1), 1 survived for 30 days and died of undetermined causes, and 5 (10.6%) are still alive at the

Downloaded from genesdev.cshlp.org on April 30, 2024 - Published by Cold Spring Harbor Laboratory Press

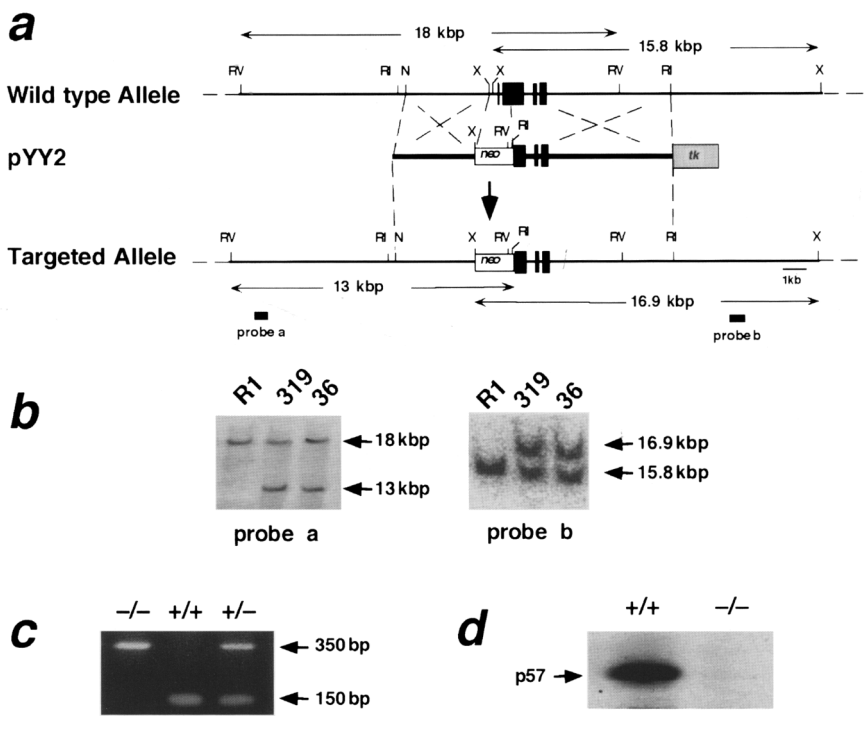

Figure 2. Generation of p57^{Kip2} (–/–) mice. (*a*) Targeting strategy. (*Top*) Partial restriction map of wild-type 129/Sv genomic DNA encompassing the four exons (solid boxes) of the *p57^{Kip2}* gene. (RI) *Eco*RI; (RV) *Eco*RV; (N) *Not*I; (X) *Xho*I. (*Middle*) The targeting vector pYY2 contains the *neo* (open box) and thymidine kinase (stippled box) genes driven by the PGK promoter. The PGK–*neo* cassette has replaced 1.1 kb of *p57^{Kip2}* genomic sequences that encompass the entire first exon as well as those nucleotides in the second exon that encode amino acid residues 1–181 of the p57^{Kip2} protein. (*Bottom*) Schematic diagram of the predicted targeted allele resulting from homologous recombination between the wild-type allele and the targeting vector. Sequences used for Southern blot analysis of recombinant ES cell clones (probes a and b) are indicated by solid bars. Probe a recognizes *Eco*RV DNA fragments of 18 kb (wild-type allele) and 13 kb (targeted allele). Probe b detects *Xho*I DNA fragments of 15.8 kb (wild-type allele) and 16.9 kb (targeted allele). (*b*) Southern blot analysis of the parental ES cells (clone R1) and of two representative recombinant clones (B302-36, B302-319) used to generate chimeric mice. Migration of *Eco*RV (probe a) and *Xho*I (probe b) DNA fragments are indicated by arrows. (*c*) PCR-aided amplification of DNAs isolated from tails of littermates derived from crosses between *p57^{Kip2}* (+/–) mice. Migration of DNA fragments derived from wild-type (150 bp) and targeted (350 bp) alleles is indicated by arrows. (*d*) Western blot analysis of primary embryo fibroblasts derived from (+/+) and (–/–) mice. The migration of the p57^{Kip2} protein is indicated by an arrow.

time of this writing (Table 1). None of the six (–/–) animals that survived beyond P1 displayed detectable morphologic or behavioral abnormalities. However, each of the 41 (–/–) mice that died shortly after birth displayed various levels of limb shortening. In addition, these mice have difficulty in suckling, as revealed by the frequent absence of milk in their stomachs. This defect could be partially explained by the presence of a cleft palate in about half of these mice (23 of 47; 48.9%) (Table 1). Most of the 23 animals with a cleft palate (16 of 23; 70%) also displayed an inflated gastrointestinal (GI) tract, suggesting inappropriate intake of air in their GI. In addition, ~40% of the (–/–) mice possessed a grossly shortened and abnormal intestine. This phenotype was observed regardless of whether the mice had cleft palate or not, suggesting that the absence of p57^{Kip2} causes developmental abnormalities in the GI tract. Finally, 1 of the 47 (–/–) mice displayed an umbilical hernia, and 4 did not present additional abnormalities.

Phenotypic defects in imprinted p57^{Kip2} *heterozygous mice*

Previous studies have demonstrated that the *p57^{Kip2}* gene is paternally imprinted (Hatada and Mukai 1995; Matsuoka et al. 1996). In humans, imprinting does not

Table 1. *Phenotypic defects observed in surviving* p57^{Kip2} *mutant mice*

Number of mice	Survival	Phenotype
Heterozygous mice (targeted paternal allele)		
80/80 (100%)	>P150	no detectable abnormalities
Heterozygous mice (targeted maternal allele)[a]		
12/40 (30.0%)	P0/P1	cleft palate/air in GI tract/short limbs
6/40 (15.0%)	P0/P1	cleft palate/short and/or disrupted intestine/short limbs
15/40 (37.5%)	P0/P1	short and/or disrupted intestine/short limbs
2/40 (10.6%)	P0/P1	no detectable abnormalities
5/40 (12.5%)	>P150	no detectable abnormalities
Homozygous mice		
16/47 (34.0%)	P0/P1	cleft palate/air in GI tract/short limbs
7/47 (14.9%)	P0/P1	cleft palate/short and/or disrupted intestine/short limbs
12/47 (25.5%)	P0/P1	short and/or disrupted intestine/short limbs
1/47 (2.1%)	P0/P1	umbilical hernia/short limbs
5/47 (10.6%)	P0/P1	short limbs
1/47 (2.1%)	P30	no detectable abnormalities
1/47 (2.1%)	>P70	no detectable abnormalities
4/47 (8.5%)	>P150	no detectable abnormalities

[a]Not all progeny was checked for limb defects.

Downloaded from genesdev.cshlp.org on April 30, 2024 - Published by Cold Spring Harbor Laboratory Press

appear to be complete, as low levels of expression of the paternal allele have been observed in certain tissues (Matsuoka et al. 1996). In mice, the paternal allele appears to be transcriptionally repressed and methylated (Hatada and Mukai 1995). As expected, none of 162 animals born from crosses between (+/−) males and (+/+) females displayed any obvious anatomical or behavioral defects. These results indicate that ablation of the paternal allele does not have significant phenotypic consequences in mice. However, when we analyzed the progeny of crosses between (+/+) males and (+/−) females, 59 (59.6%) of 99 live births were (+/+) and only 40 (40.4%) were (+/−), suggesting that targeting of the maternal allele results in partial embryonic lethality. More importantly, 35 of the 40 (+/−) animals that inherited the maternal allele died within their first day of life, a percentage very similar to that observed in the *null* (−/−) mutants. None of these (+/−) mice had detectable milk in their stomachs and they displayed the same anatomical defects as the (−/−) mice, including short limbs, cleft palate, and intestinal abnormalities (Table 1). Five (+/−) mice carrying a targeted maternal allele have survived without apparent defects for at least 6 months, a similar proportion of mice observed in those with a *null* genotype (Table 1). These results support the notion that the paternal allele is completely imprinted in mice.

Defective palate formation in p57^{Kip2} null *mice*

The cleft palate observed in (−/−) and imprinted (+/−) mice had defects in both the hard and soft palate (Fig. 3). Palatal development is a complex process that involves fine-tuned interactions between the epithelial and mesenchymal cells (Ferguson 1988). During early embryonic stages, the oral and nasal cavities form a single compartment. At E12.5, bilateral palatal shelves arise from the maxillary process of the first branchial arch (Ferguson 1988; Kaufman 1992). The palatal shelves grow, first downward along the sides of the tongue and then upward to a horizontal position. Subsequently, they extend toward the midline, meet, and fuse above the tongue. As a result, the oral and nasal cavities are separated. Developmental defects in which the two palatal shelves fail to grow and meet in the midline, or fail to fuse completely, result in cleft palate in which the oral and nasal cavities remain connected.

Close examination of the *p57^{Kip2}* (−/−) mice with cleft palate suggests that the two palatal shelves have failed to grow and meet at the midline, indicating a defect in the growth of the palatal shelves (Fig. 3e). To determine the possible cause of this impaired growth, we examined palate formation at E14.5, a time at which the palatal shelves are in the process of growing toward the midline (Ferguson 1988; Kaufman 1992). In these embryos, p57^{Kip2} is expressed in the palatal shelves, both in epithelial cells on the surface and in the mesenchymal cells located deep in the shelves (data not shown). Analysis of E14.5 (−/−) embryos by the terminal deoxynucleotide transferase (TdT)-mediated dUTP–biotin nick-end labeling (TUNEL) assay revealed a significant number of apoptotic epithelial cells on the surface of the palatal shelves (Fig. 3f,g). In contrast, very few apoptotic cells were observed in the same region of their (+/+) littermates (Fig. 3b,c). Likewise, we observed increased apoptosis in the mesenchyme located at the base of the palatal shelves in the (−/−) mutant animals (Fig. 3h). Whereas it is not possible to determine whether the cells undergoing apoptosis in the palatal shelves of *p57^{Kip2}* (−/−) mice are those that express p57^{Kip2} in wild-type animals, it is tempting to hypothesize that the absence of p57^{Kip2} in these cells may fail to regulate their exit from the cell cycle and trigger apoptosis.

Disruption of the p57^{Kip2} *gene causes developmental defects in the gastrointestinal tract*

As indicated above, ~75% of the (−/−) mice that die dur-

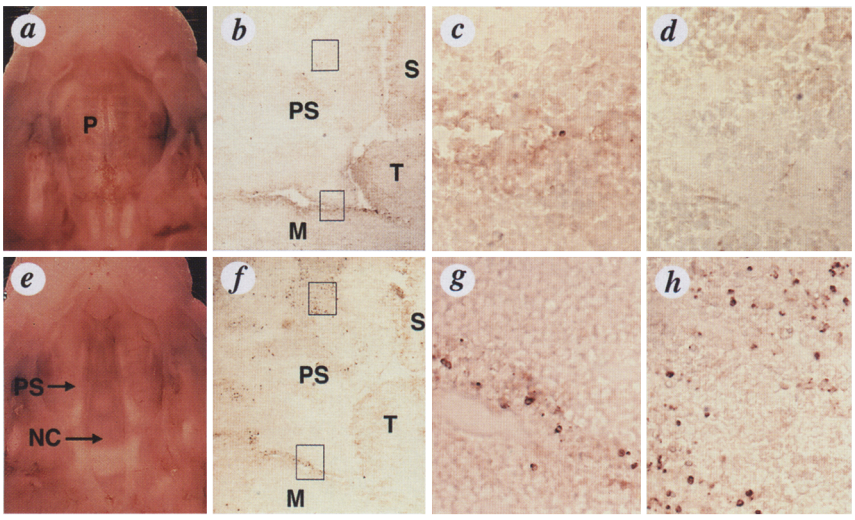

Figure 3. Palatogenesis in wild-type (*a–d*) and *p57^{Kip2}* (*e–h*) mutant mice. (*a*) Normal fused palate (P); (*e*) cleft palate. The palatal shelves (PS) do not grow toward the midline leaving the nasal cavity (NC) connected with the oral cavity. TUNEL assay of comparable frontal sections of the snout of (+/+) (*b*) and (−/−) (*f*) E14.5 embryos. At this time, the palatal shelves (PS) are in the process of growing toward the midline. The tongue (T), which is underneath the nasoseptum (S), will later move downward so that palatal shelves will meet above the tongue. (M) mandible. Few apoptotic nuclei are observed among the epithelial cells (*c*) on the surface of palatal shelves (lower square in *b*) or among the mesenchymal cells (*d*) inside the palatal shelves (upper square in *b*) of the (+/+) mouse. However, there are abundant apoptotic figures in the corresponding regions (*g,h*, respectively) of (−/−) mice.

Downloaded from genesdev.cshlp.org on April 30, 2024 - Published by Cold Spring Harbor Laboratory Press

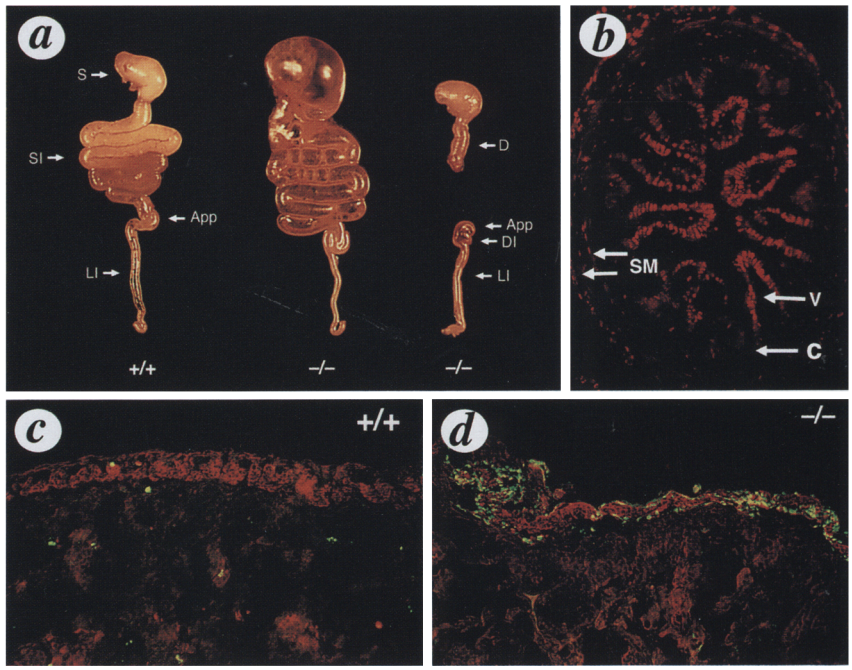

Figure 4. Defects in the gastrointestinal tract of *p57^{Kip2}* mutant mice. (*a*) GI tracts of neonatal (*left*) (+/+) and (−/−) mice displaying either inflated stomach and small intestine (*middle*) or a grossly abnormal and disrupted small intestine (*right*). (App) Appendix; (D) duodenum; (DI) distal ileum; (LI) large intestine; (S) stomach; (SI) small intestine. (*b*) Expression of p57^{Kip2} in the small intestine. Robust p57^{Kip2} immunoreactivity can be observed in the differentiated cells of the apical region of the villi (V) but not in the dividing cells of the crypts (C). p57^{Kip2} expression could also be detected in the smooth muscle cells (SM) of the intestinal wall. (*c*,*d*) Double-labeling of cross sections from the small intestine of (+/+) (*c*) and (−/−) (*d*) mice with TUNEL assay (green fluorescence) and polyclonal antibodies against smooth muscle-specific MLCK (red fluorescence). Sections from (−/−) mice correspond to an area near disrupted small intestine tissue.

ing early postnatal development (P0/P1) have defects in their GI tracts (Table 1). Some of these mutant animals display inflated stomachs and small intestines because of the presence of air bubbles (Fig. 4a). Histological analysis did not reveal gross pathological defects in the GI tract of these mice, except for a significant stretching of the tissues presumably attributable to the pressure exerted by the air bubbles (data not shown). As indicated above, it is likely that the lack of separation between the oral and nasal cavities in animals with a cleft palate contributes to the accumulation of air bubbles by misrouting air to the GI tract. However, it is also possible that this phenotype might be caused by a defect in peristaltic movements, an activity regulated by the enteric and sympathetic nervous systems. To examine this possibility, tissue sections were incubated with antibodies against PGP9.5 and tyrosine hydroxylase, two markers that stain enteric neurons and sympathetic nerve fibers, respectively. No significant defects could be observed in either type of neurons (data not shown).

More than half of the (−/−) mice that died at P0/P1 have developmental GI defects. The stomach and duodenum of these mice appeared grossly normal; however, most of their jejunum and ileum was absent (Fig. 4a). The duodenum ended blindly and was open to the abdominal cavity. At the blind ends of the duodenum and distal ileum, there was hemorrhage in the intestinal wall, suggesting tissue degeneration. In the intestine, the p57^{Kip2} protein is expressed in the differentiated cells of the apical region of the villi as well as in the smooth muscle cells of the GI wall (Fig. 4b). To determine whether any of these regions may undergo increased apoptosis as a consequence of the absence of p57^{Kip2}, we carried out TUNEL assays on sections from these intestinal regions of (+/+) and (−/−) P0 mice. The overall level of apoptosis in the villi and intestinal wall of the (−/−) animals was higher than in the same regions of their (+/+) littermates (data not shown). Moreover, there was massive apoptosis in those regions near the ends of the disconnected intestines (Fig. 4d). Double staining of these sections with an antibody elicited against the smooth muscle-specific myosin light-chain kinase (MLCK) indicated that the observed apoptosis was restricted to the smooth muscle cell layer of the intestinal wall (Fig. 4d). Examination of the same regions in those (−/−) mice that do not display disruption of their small intestines failed to reveal this massive increase in apoptosis. Therefore, it is not clear whether the high levels of apoptotic cell death in the intestinal wall is cause or consequence of the disruption of the small intestine observed in some (−/−) animals. Finally, no obvious abnormalities or significant increase in apoptotic figures could be observed in the intestine of E15.5 (−/−) embryos, indicating that the degeneration of the intestine in *p57^{Kip2}* mutant mice occurs during the late stages of embryonic development.

Defective endochondral bone formation in p57^{Kip2} *(−/−) mice*

Postnatal (P0/P1) *p57^{Kip2}* (−/−) mice have consistently shorter limbs than their wild-type littermates (Fig. 5a). To examine whether there was a defect in skeletal formation in these mutant mice, we stained P0 mice with alcian blue and alizarin red, two dyes specific for cartilage and bone, respectively (Kaufman 1992). The overall structure of the skeleton of the (−/−) mice appeared nor-

Downloaded from genesdev.cshlp.org on April 30, 2024 - Published by Cold Spring Harbor Laboratory Press

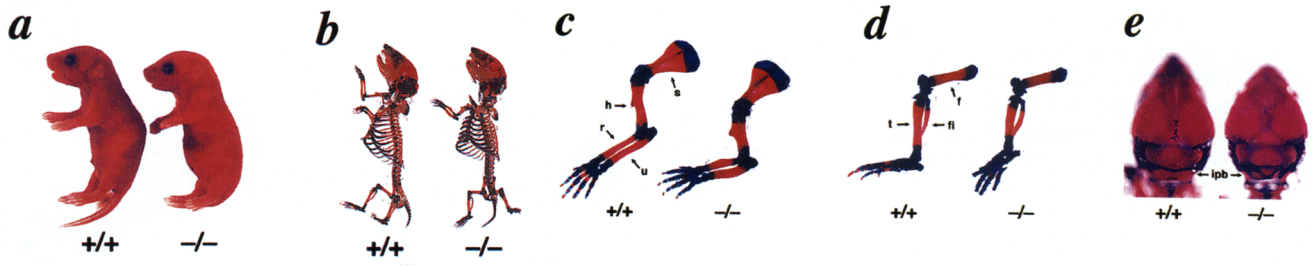

Figure 5. Defective endochondral bone formation in *p57^{Kip2}* mutant mice. (*a*) External appearance of (+/+) and (–/–) neonatal mice. (*b*) Skeleton preparation of whole body from P0 mice stained with alcian blue and alizarin red. Forelimbs (*c*) and hindlimbs (*d*) of neonatal mice. (s) Scapula; (h) humerus; (r) radius; (u) ulna; (f) femur; (t) tibia; (fi) fibula. The bones are significantly shorter in the mutant animals. Cartilages appear to be longer in the humerus (h) and the digits. (*e*) Posterior view of the skull. The interparietal bones (ipb) in the (–/–) mice appear to be underdeveloped with three ossification centers, indicated by three areas of red color separated by blue-colored cartilage. In the interparietal bone of the (+/+) mouse, the three ossification centers had already become one, indicating a more advanced developmental stage. The genotype of each mouse is indicated.

mal (Fig. 5b). However, the ossified part of their bones was substantially shorter, resulting in shorter limbs despite having a slightly longer cartilaginous region (Fig. 5c,d). This defect is specific for those bones formed through endochondral ossification, as most cranial bones, which develop through intramembranous ossification, appeared to be normal (Fig. 5e). In support to this concept, the interparietal bone that forms at the base of the skull through endochondral ossification is also significantly underdeveloped in the *p57^{Kip2}* (–/–) mice (Fig. 5e).

During the initial stages of endochondral ossification, the chondrocytes located in the cartilage, the tissue that forms the scaffold of the bone, are at resting stage. Later in the development, they proliferate, undergo hypertrophy, and stop dividing. Finally, they are calcified and replaced by the invading osteocytes, which form the mature bone tissue. Histological analysis of the long bones in the limbs of the *p57^{Kip2}* mutant mice indicates that the chondrocytes undergo hypertrophy at a greater distance from the epiphysis than in the wild-type mice (Fig 6a,c), suggesting that the terminal differentiation of the chondrocytes is delayed in the absence of p57^{Kip2}. Immunohistochemical analysis revealed that whereas resting and proliferating chondrocytes express low to moderate levels of p57^{Kip2}, hypertrophic chondrocytes undergoing terminal differentiation express high levels of p57^{Kip2} (Fig. 6b). This pattern of expression suggests that p57^{Kip2} plays a role in chondrocyte differentiation. In the absence of p57^{Kip2}, chondrocytes undergo a delay in differentiation which, in turn, causes a decrease in the space in which the osteocytes can be formed, resulting in shorter bones. No defect in osteoclast formation was observed in *p57^{Kip2}* (–/–) animals (data not shown).

In support of this hypothesis, the density of chondrocytes in the epiphysis of long bones is significantly higher (46%) in the (–/–) than in the (+/+) mice (Fig. 7a). The increase in chondrocyte numbers may be the result of increased proliferation or decreased cell death. To distinguish between these two possibilities, we carried out a TUNEL assay. No significant apoptosis was found in the epiphysis from either *p57^{Kip2}* (–/–) or wild-type mice (data not shown). However, when E16.5 embryos were labeled with BrdU, almost twice as many chondrocytes became labeled in the (–/–) embryos (15%) than in their (+/+) littermates (8%) (Fig. 7b). Taken together, these results, indicate that p57^{Kip2} has a key role in the differentiation of chondrocytes by regulating their exit from the cell cycle.

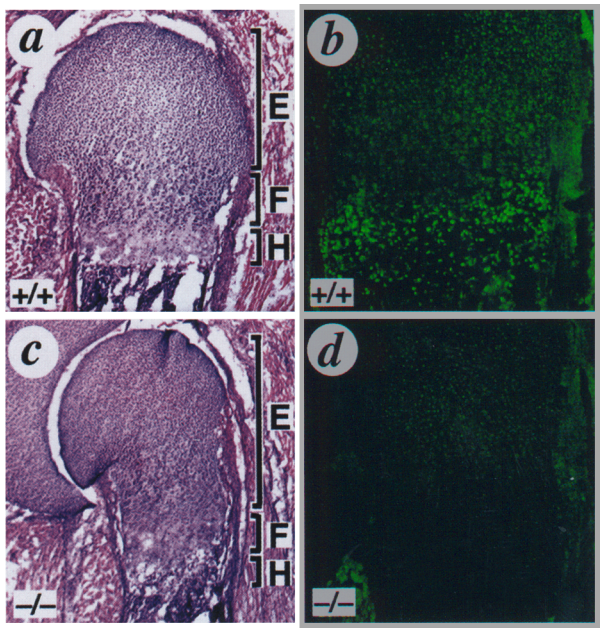

Figure 6. Delayed chondrocyte differentiation in *p57^{Kip2}* mutant mice. (*a,c*) Hematoxylin and eosin staining of longitudinal sections proximal to the humerus growth plate from P0 (+/+) (*a*) and (–/–) (*c*) mice. (E) Epiphysis; (F) zone of flattened cells; (H) zone of hypertrophic cells. Chondrocytes undergo hypertrophy at a greater distance from the epiphysis in the (–/–) than in the (+/+) animals. (*b,d*) p57^{Kip2} expression in sections adjacent to those shown in *a* and *c*, respectively. The hypertrophic cells of the (+/+) mouse are strongly labeled, whereas the cells in the epiphysis and the proliferation zone are stained at lower intensity. No detectable signal can be seen in the section derived from the (–/–) mouse.

Downloaded from genesdev.cshlp.org on April 30, 2024 - Published by Cold Spring Harbor Laboratory Press

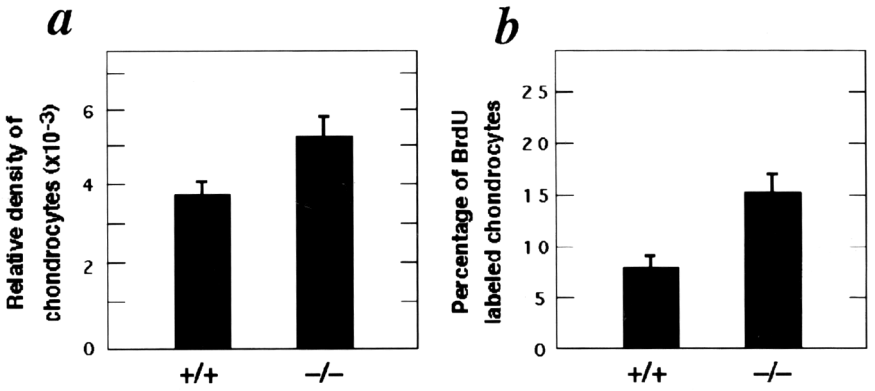

Figure 7. (*a*) Quantification of chondrocyte density in the epiphysis of neonatal mice. The number of chondrocyte nuclei were counted within a defined area of hematoxylin- and eosin-stained sections (10 μm thick), and the number raised exponentially to the power 3/2 to make it three-dimensional. (*b*) Percentage of proliferating chondrocytes in the proximal epiphyseal center of the humerus in E16.5 embryos as determined by BrdU labeling. The total number of chondrocyte nuclei as well as the number of BrdU-labeled chondrocyte nuclei were counted within a defined area from two sections. Each bar represents the average counts of three animals. Error bars represent the standard error.

Discussion

Targeted disruption of the *p57^{Kip2}* gene results in developmental abnormalities. These observations are in contrast to those obtained with mice carrying homozygous disruptions in genes encoding other Cdk inhibitors such as *p16^{Ink4a}* (Serrano et al. 1996), *p21$^{Cip/WAF1}$* (Deng et al. 1995), *p27^{Kip1}* (Fero et al. 1996; Kiyokawa et al. 1996; Nakayama et al. 1996), *p15^{Ink4b}*, and *p18^{Ink4c}* (E. Latres and M. Barbacid, unpubl.), in which no significant developmental defects have been observed. Furthermore, characterization of the *p57^{Kip2}* (–/–) mice suggests that p57^{Kip2} plays a unique role in controlling critical steps that determine the exit from the cell cycle during embryonic development. These observations are reminescent of the the role that the *Drosophila dacapo* gene, another member of the Cip/Kip family of Cdk inhibitors, plays during *Drosophila* embryogenesis (de Noolj et al. 1996; Lane et al. 1996).

Accumulating evidence indicates that alterations in the orderly progression through cell cycle checkpoints often trigger apoptotic events (El-Deiry et al. 1994; Lee et al. 1994; Field et al. 1996). Increased apoptosis in the growing palatal shelves of *p57^{Kip2}* (–/–) mice is likely to be responsible for the formation of a cleft palate in about half of these animals. Unscheduled apoptosis is also likely to be responsible for the shortened intestines found in the targeted *p57^{Kip2}* mice, as those areas surrounding the missing GI tract display massive levels of apoptotic figures. Whether this apoptosis is directly caused by the lack of p57^{Kip2} protein in GI tissue or results as a consequence of another physiological defect remains to be determined. However, the presence of an apparently normal enteric nervous system makes it unlikely that the observed apoptosis is caused by defective innervation. *p57^{Kip2}* mutant mice also display increased levels of apoptotic cells in other tissues with high levels of p57^{Kip2} expression such as cardiac and skeletal muscle (Y. Yan, J. Frisén, and M. Barbacid, unpubl.). However, no significant anatomical defects have been observed in these tissues, suggesting that the increased apoptosis is either compensated or not sufficient to alter their homeostasis. The existence of defects in the lens as well as in components of the hematopoietic and nervous systems is currently under investigation.

Mice lacking *p57^{Kip2}* display rather variable levels of penetrance. For instance, a limited, albeit significant, percentage of *p57^{Kip2} null* mice (~10%) survive without any obvious abnormalities, and only half of the mutant animals have a cleft palate. Likewise, disruption of the GI tract only occurs in about one-third of the homozygous targeted animals and only encompasses a limited (and variable) region of the intestine. Analysis of the morphologically normal areas of the GI tract in those (–/–) mice showing a disrupted GI tract did not reveal significantly increased levels of apoptosis, thus indicating that massive apoptotic cell death only occurs in localized regions of the intestine. The molecular bases for the variable penetrance observed in mice lacking p57^{Kip2} protein remain to be established. However, it is likely to be a consequence of the complex feedback circuits that control the progression and exit from the cell cycle.

p57^{Kip2} null mice display short limbs, a defect attributable to shortening of their limb bones. These bones have a larger cartilaginous region but a shorter ossified area, resulting in a diminished overall length. In addition, all of the *p57^{Kip2} null* mice analyzed in this study have an underdeveloped interparietal bone but no defects in any of the other cranial bones. The cartilaginous region of these bones in p57^{Kip2} (–/–) mice has elevated numbers of chondrocytes, a likely consequence of their increased proliferation. Moreover, histological analysis of the long bones of these mutant animals indicates that their chondrocytes undergo hypertrophy at a greater distance from the epiphysis than in their wild-type littermates. These observations are consistent with the idea that p57^{Kip2} plays an important role in the regulation of cell cycle exit and differentiation in chondrocytes. In the absence of p57^{Kip2}, chondrocytes experience a delay in cell cycle withdrawal and do not become hypertrophic in a timely fashion, thus resulting in fewer cells undergoing terminal differentiation. In normal mice, chondrocytes in the epiphysis express low to moderate levels of p57^{Kip2} protein. However, the levels of p57^{Kip2} increase greatly in those distal regions where chondrocytes become hypertrophic. The temporal correlation between

Downloaded from genesdev.cshlp.org on April 30, 2024 - Published by Cold Spring Harbor Laboratory Press

chondrocyte differentiation and up-regulation of p57^{Kip2} expression, along with the phenotype displayed by those bones of *p57^{Kip2} null* mice formed by endochondral ossification, strongly suggests that p57^{Kip2} has a critical role in regulating chondrocyte differentiation.

The endochondral ossification defect observed in *p57^{Kip2} null* mice bears a high resemblance to that observed in mice defective for p107 and p130, two members of the retmoblastoma (Rb) family of proteins (Cobrinik et al. 1996). Rb, p107, and p130 are structurally related molecules that differ in their specificity for binding to the E2F family of transcription factors (Weinberg 1995). In p107/p130 double mutant mice, the chondrocyte density is higher than in either single mutant or wild-type littermates. BrdU labeling experiments similar to those performed with *p57^{Kip2} null* mice also suggest that the higher density of chondrocytes in these mice is attributable to a deregulated cell cycle (Cobrinik et al. 1996). Moreover, the p107/p130-defective chondrocytes experience a delay in differentiation similar to that seen in chondrocytes lacking the p57^{Kip2} protein. These observations raise the possibility that p57^{Kip2} regulates those cyclin–Cdk complexes responsible for the phosphorylation of p107 and p130.

The *p57^{Kip2}* gene maps at 11p15, a chromosomal region that contains paternally imprinted genes likely to be involved in the development of embryonic tumors as well as in the Beckwith–Wiedemann syndrome, a genetic defect characterized by various growth abnormalities such as macroglossia, gigantism, and visceromegaly (Cohen and Gorlin 1971; Eaton and Maurer 1971; McNamara et al. 1972). Beckwith–Wiedemann syndrome patients also have a high risk of developing childhood tumors (Wiedemann 1983). The possible involvement of *p57^{Kip2}* in the development of the Beckwith–Wiedemann syndrome has been substantiated by the identification of two Beckwith–Wiedemann syndrome patients carrying mutated *p57^{Kip2}* genes (Hatada et al. 1996; Kondo et al. 1996). The *p57^{Kip2}* gene has also been implicated in the development of certain human tumors. For instance, *p57^{Kip2}* transcripts in Wilms' tumors are only 5%–10% of those found in matched normal kidney tissue from the same patients (Thompson et al. 1996). Moreover, the functional maternal *p57^{Kip2}* allele has been found to be selectively lost in 11 of 13 lung carcinomas carrying 11p15 deletions (Kondo et al. 1996).

Our results confirm previous observations indicating that the mouse *p57^{Kip2}* locus is paternally imprinted (Hatada and Mukai 1995). Heterozygous mice derived from crosses between wild-type males and *p57^{Kip2}* (+/−) females display the same incidence of developmental defects as the *null p57^{Kip2}* (−/−) animals, indicating that the penetrance of the imprinted *p57^{Kip2}* allele in mice is complete, at least in the affected tissues. However, *p57^{Kip2}* mutant mice do not exhibit the phenotypic characteristics of patients with Beckwith–Wiedemann syndrome. It is possible that mutations in the *p57^{Kip2}* gene have somewhat different phenotypic consequences in mice and humans, as observed previously with other tumor suppressor genes such as *Rb* (Jacks et al. 1992; Lee et al. 1992). In addition, we have not observed tumors in these *p57^{Kip2}* mutant animals. However, increased numbers of surviving homozygous mice will be necessary to fully assess the role of the *p57^{Kip2}* gene in neoplastic development.

In summary, we report that elimination of the cell cycle regulator p57^{Kip2} causes significant developmental abnormalities most likely to result from increased apoptosis and delayed differentiation. However, the phenotypic consequences of targeting the *p57^{Kip2}* gene could only be observed in a subset of cells that normally express this protein. Moreover, the penetrance of the developmental defects of *p57^{Kip2} null* mice varies tremendously, as some of these mutant animals develop normally. These observations illustrate the complex nature of the circuits that control the mammalian cell cycle and underscore the importance of studying the role of individual cell cycle regulators in vivo.

Materials and methods

Generation of p57^{Kip2} *mutant mice*

The targeting vector pYY2 was generated by subcloning a 4.0-kb *Not*I–*Xho*I DNA fragment of genomic 129/Sv DNA encompassing sequences upstream of the four exons of the *p57^{Kip2}* gene into the *Not*I and *Xho*I sites of the pPNT plasmid (left arm) and a 7.5-kb *Eco*RI DNA fragment of genomic 129/Sv DNA that contains part of the second exon as well as the entire third and fourth exons of the *p57^{Kip2}* gene (amino acid residues 182–348) in the *Eco*RI site of pPNT (right arm) (Fig. 2) (Tybulewick et al. 1991). pYY2 DNA was transfected into R1 ES cells as described previously (Joyner 1993). G418^{R}/Gan^{R} ES cell clones were analyzed by Southern blot using as probes a 0.6-kb *Hin*dIII DNA fragment (probe a) and a 0.7-kb *Eco*RI–*Hin*dIII DNA fragment (probe b) derived from genomic 129/Sv DNA sequences (Fig. 2a). G418^{R}/Gan^{R} ES cell clones carrying a targeted *p57^{Kip2}* allele were either microinjected into C57BL/6 mouse blastocysts (clone B302-319) or aggregated with morula cells from ICR mice (clones B302-36 and B302-319). Chimeras derived from these clones transmitted the targeted allele when bred to wild-type C57BL/6 and ICR mice, respectively. The resulting heterozygous mice were subsequently bred to the corresponding strain of mice to propagate the mutant allele or among themselves to generate homozygous mice. Mice were routinely genotyped by submitting DNA isolated from tail clips to PCR-aided amplification using primers specific for either the wild-type (*p57^{Kip2}* sequences corresponding to amino acid residues 49–98 that were deleted during homologous recombination; YY11, ATGCGCCTGGCCGAGCTGAA, and YY12, CGGTAGAAGGCGGGCACAGA) or the targeted (*neo* sequences, BH81, GAGGCTATTCGGCTATGA, and BH82, ATGTTTCGCTTGGTGGTC) allele. YY11 and YY12 amplify a DNA fragment of 150 bp, whereas BH81 and BH82 amplify a DNA fragment of 350 bp (Fig. 2c).

Western blot analysis

Mouse embryo fibroblasts (MEFs) were obtained and cultured as described previously (Deng et al. 1995). Cells were lysed in RIPAE buffer (10 mM Tris-HCl at pH 8.0, 0.1% Triton X-100, 150 mM NaCl, 1% aprotinin, 250 μM PMSF), and the lysate was quantified with a Bio-Rad Kit following the conditions suggested by the manufacturer. Proteins (50 μg) were loaded onto a 10% SDS–polyacrylamide gel and subjected to electrophoresis.

Downloaded from genesdev.cshlp.org on April 30, 2024 - Published by Cold Spring Harbor Laboratory Press

Electrophoresed proteins were transferred to an Immobilon membrane (Millipore, Bedford, MA) and probed with a polyclonal rabbit antiserum (no. 522) elicited against peptide PP3 (AQENKASNDVPPGCPSPN, corresponding to amino acid residues 314–331 of $p57^{Kip2}$). Immunocomplexes were visualized by enhanced chemiluminescence (Amersham, Arlington Heights, IL) using goat anti-rabbit IgG antibodies coupled to horseradish peroxidase (Amersham).

Histological analysis

Fixed frozen tissues were sectioned at 10 μm thickness. Sections were incubated in blocking solution (0.3% Triton X-100, 2% BSA in PBS) for 10 min followed by incubation (37°C for 1 hr) with anti-$p57^{Kip2}$ antibodies (1:100 dilution in blocking solution). Sections were washed three times with PBS and incubated (at room temperature for 1 hr) with rhodamine-conjugated bovine anti-rabbit IgG antiserum.

TUNEL assay

Tissues were fixed overnight in 4% paraformaldehyde buffered with PBS, incubated overnight in a 10% sucrose solution in PBS, embedded in OTC, and sectioned at 10 μm thickness. An ApopTag kit (Oncor, Gaithersburg, MD) was used to carry out the TUNEL assay following the conditions suggested by the manufacturer.

Bone and cartilage staining

Skeletal preparations were carried out as described previously (Kessel and Gruss 1991). Briefly, newborn mice were eviscerated, fixed in 100% ethanol for 4 days, kept in acetone for 3 days, and rinsed with water. Bones and cartilage tissue were stained for 10 days in staining solution consisting of 1 volume of 0.3% alcian blue 8GX (Sigma) in 70% ethanol, 1 volume of 0.1% alizarin red S (Sigma) in 95% ethanol, 1 volume of 100% acetic acid, and 17 volumes of ethanol. Tissues were kept in 20% glycerol and 1% potassium hydroxide at 37°C for 16 hr, and then at room temperature until they had cleared completely. For storage, specimens were transferred to 50%, 80%, and finally 100% glycerol.

BrdU staining

For BrdU labeling experiments, heterozygous females (16.5 dpc) were injected intraperitoneally with 1 ml of 100 mg/ml BrdU in 0.9% NaCl. Animals were sacrificed 1 hr later and the embryos collected. Tissues were fixed overnight in 4% paraformaldehyde buffered with PBS, incubated overnight in a 10% sucrose solution in PBS, embedded in OTC, and sectioned at 10 μm thickness. Staining was carried out using a BrdU staining kit (Calbiochem, Cambridge, MA) according to conditions recommended by the manufacturer.

Acknowledgments

We are indebted to the staff of the Transgenic Unit for their help in generating the $p57^{Kip2}$ mutant mice. We also thank Inmaculada Silos-Santiago for valuable discussions and Johnni Gullo-Brown and Linda Long for excellent technical assistance. J.F. was supported by the Wenner-Gren Foundations.

The publication costs of this article were defrayed in part by payment of page charges. This article must therefore be hereby marked "advertisement" in accordance with 18 USC section 1734 solely to indicate this fact.

References

Brugarolas, J., C. Chandrasekaran, J.I. Gordon, D. Beach, T. Lacks, and G.J. Hannon. 1995. Radiation-induced cell cycle arrest compromised by p21 deficiency. *Nature* **377:** 552–557.

Cobrinik, D., M.-H. Lee, G. Hannon, G. Mulligan, R.T. Bronson, N. Dyson, E. Harlow, D. Beach, R.A. Weinberg, and T. Jacks. 1996. Shared role of the pRB-related p130 and p107 proteins in limb development. *Genes & Dev.* **10:** 1633–1644.

Cohen, M.M. and R.J. Gorlin. 1971. The Beckwith-Wiedemann syndrome. *Am. J. Dis. Child.* **122:** 515–519.

Datto, M.B., Y. Li, J.F. Panus, D.J. Howe, Y. Xiong, and X.-F. Wang. 1995. Transforming growth factor β induces the cyclin-dependent kinase inhibitor p21 through a p53-independent mechanism. *Proc. Natl. Acad. Sci.* **92:** 5545–5549.

de Noolj, J.C., M.A. Letendre, and I.K. Hariharan. 1996. A cyclin-dependent kinase inhibitor, Dacapo, is necessary for timely exit from cell cycle during Drosophila embryogenesis. *Cell* **87:** 1237–1247.

Deng, C., P. Zhang, J.W. Harper, S.J. Elledge, and P. Leder. 1995. Mice lacking $p21^{Cip1/WAF1}$ undergo normal development, but are defective in G1 checkpoint control. *Cell* **82:** 675–684.

Eaton, A.P. and W.F. Maurer. 1971. The Beckwith-Wiedemann syndrome. *Am. J. Dis. Child.* **122:** 520–525.

El-Deiry, W.S., J.W. Harper, P.M. O'Connor, V. Velculescu, C.E. Canman, J. Jackman, J. Pietenpol, M. Burell, D.E. Hill, W.E. Mercer, M.B. Kastan, K.W. Kohn, S.J. Elledge, K.W. Kinzler, and B. Volgelstein. 1994. WAF1/CIP1 is induced in p53-mediated G1 arrest and apoptosis. *Cancer Res.* **54:** 1169–1174.

Ferguson, M.W.J. 1988. Palate development. *Development* (Suppl.) **103:** 41–60.

Fero, M.L., M. Rivkin, M. Tasch, P. Porter, C.E. Carow, E. Firpo, K. Polyak, L.-H. Tsai, V. Broudy, R.M. Perlmutter, K. Kaushansky, and J.M. Roberts. 1996. A syndrome of multiorgan hyperplasia with features of gigantism, tumorigenesis, and female sterility in $p27^{Kip1}$-deficient mice. *Cell* **85:** 733–744.

Field, S., F.-Y. Tsai, F. Kuo, A.M. Zubiaga, W.G. Kaelin, Jr., D.M. Livingston, S.H. Orkin, and M.E. Greenberg. 1996. E2F-1 functions in mice to promote apoptosis and suppress proliferation. *Cell* **85:** 549–561.

Hall, M. and G. Peters. 1996. Genetic alterations of cyclins, cyclin-dependent kinases and cdk inhibitors in human cancer. *Adv. Cancer Res.* **68:** 67–108.

Hannon, G.J. and D. Beach. 1994. $p15^{INK4B}$ is a potential effector of TGF-β-induced cell cycle arrest. *Nature* **371:** 257–261.

Harper, J.W., G.R. Adami, N. Wei, K. Keyomarsi, and S.J. Elledge. 1993. The p21 cdk-interacting protein Cip1 is a potent inhibitor of G1 cyclin-dependent kinases. *Cell* **75:** 805–816.

Hatada, I. and T. Mukai. 1995. Genomic imprinting of $p57^{Kip2}$, a cyclin-dependent kinase inhibitor, in mouse. *Nature Genet.* **11:** 204–206.

Hatada, I., H. Ohashi, Y. Fukushima, Y. Kaneko, M. Inoue, Y. Komoto, A. Okada, S. Ohishi, A. Nabetani, H. Morisaki, M. Nakayama, N. Niikiwa, and T. Mukai. 1996. An imprinted gene $p57^{Kip2}$ is mutated in Beckwith-Wiedemann syndrome. *Nature Genet.* **14:** 171–173.

Havely, O., B.G. Novitch, D.B. Spicer, S.X. Skapek, J. Rhee, G.J. Hannon, D. Beach, and A. Lassar. 1995. Correlation of terminal cell cycle arrest of skeletal muscle with induction of p21 by MyoD. *Science* **267:** 1018–1021.

Hunter, T. and J. Pines. 1994. Cyclins and cancer II: Cyclin D and CDK inhibitiors come of age. *Cell* **79:** 573–582.

Jacks, T., A. Fazeli, E.M. Schmitt, R.T. Bronson, M.A. Goodell, and R.A. Weinberg. 1992. Effects of an Rb mutation in the mouse. *Nature* **359:** 295–300.

Downloaded from genesdev.cshlp.org on April 30, 2024 - Published by Cold Spring Harbor Laboratory Press

Joyner, A.L. 1993. Production of targeted embryonic stem cell clones. In *Gene targeting. A practical approach* (ed. D. Rickwood and B.D. Hames), pp. 33–61. Oxford Press, Oxford, UK.

Kato, J., M. Matsuoka, K. Polyak, J. Massagué, and C.J. Sherr. 1994. Cyclic AMP-induced G1 phase arrest mediated by an inhibitor (p27^{Kip1}) of cyclin-dependent kinase-4 activation. *Cell* **79:** 487–496.

Kaufman, M.H. 1992. *The atlas of mouse development.* Academic Press, San Diego, CA.

Kessel, M. and P. Gruss. 1991. Homeotic transformations of murine vertebrae and concomitant alteration of Hox codes induced by retinoic acid. *Cell* **67:** 89–104.

Kiyokawa, H., R.D. Kineman, K.O. Manova-Todorova, V.C. Soares, E.S. Hoffmann, M. Ono, D. Khanam, A.C. Hayday, L.A. Frohman, and A. Koff. 1996. Enhanced growth of mice lacking the cyclin-dependent kinase inhibitor function of p27^{Kip1}. *Cell* **85:** 721–732.

Klein, R., R.J. Smeyne, W. Wurst, L.K. Long, B.A. Auerbach, A.L. Joyner, and M. Barbacid. 1993. Targeted disruption of the trkB neurotrophin receptor gene results in nervous system lesions and neonatal death. *Cell* **75:** 113–122.

Kondo, M., S. Matsuoka, K. Uchida, H. Osada, M. Nagatake, K. Takagi, J.W. Harper, T. Takahashi, S.J. Elledge, and T. Takahashi. 1996. Selective maternal-allele loss in human lung cancers of the maternally expressed p57^{Kip2} gene at 11p15.5. *Oncogene* **12:** 1365–1368.

Lane, M.E., K. Sauer, K. Wallace, Y.N. Jan, C.F. Lehner, and H. Vaessin. 1996. Dacapo, a cyclin-dependent kinase inhibitor, stops cell proliferation during Drosophila development. *Cell* **87:** 1225–1235.

Lee, E.Y.-H.P., C.-Y. Chang, N. Hu, Y.-C.J. Wang, C.-C. Lai, K. Herrup, W.-H. Lee, and A. Bradley. 1992. Mice deficient for Rb are nonviable and show defects in neurogenesis and haematopoiesis. *Nature* **359:** 288–294.

Lee, E.Y.-H.P., N. Hu, S.-S.F. Yuan, L.A. Cox, A. Bradley, W.-H. Lee, and K. Herrup. 1994. Dual roles of the retinoblastoma protein in cell cycle regulation and neuron differentiation. *Genes & Dev.* **8:** 2008–2021.

Lee, M.-H., I. Reynisdóttir, and J. Massagué. 1995. Cloning of p57^{Kip2}, a cyclin-dependent kinase inhibitor with unique domain structure and tissue distribution. *Genes & Dev.* **9:** 639–649.

Lee, M.-H., M. Nikolic, C.A. Baptista, E. Lai, L.-H. Tsai, and J. Massagué. 1996. The brain-specific activator p35 allows Cdk5 to escape inhibition by p27^{Kip1} in neurons. *Proc. Natl. Acad. Sci.* **93:** 3259–3263.

Liu, M., M.-H. Lee, M. Cohen, M. Bommakanti, and L.P. Freedman. 1996. Transcriptional activation of the Cd inhibitor p21 by vitamin D3 leads to the induced differentiation of the myelomonocytic cell line U937. *Genes & Dev.* **10:** 142–153.

Matsuoka, S., M.C. Edwards, C. Bai, S. Parker, P. Zhang, A. Baldini, J.W. Harper, and S.J. Elledge. 1995. p57^{Kip2}, a structurally distinct member of the p21^{Cip1} Cdk inhibitor family, is a candidate tumor suppressor gene. *Genes & Dev.* **9:** 650–662.

Matsuoka, S., J.S. Thompson, M.C. Edwards, J.M. Barletta, P. Grundy, L.M. Kalikin, J.W. Harper, S.J. Elledge, and A. Feinberg. 1996. Imprinting of the gene encoding a human cyclin-dependent kinase inhibitor, p57^{Kip2}, on chromosome 11p15. *Proc. Natl. Acad. Sci.* **93:** 3026–3030.

McNamara, T.O., C.A. Gooding, S.L. Kaplan, and R.E. Clark. 1972. Exomphalos-macroglossia-gigantism (viceromegaly) syndrome. *Am. J. Roentgenol.* **114:** 264–267.

Nakayama, K., N. Ishida, M. Shirane, A. Inomata, T. Inoue, N. Shishido, I. Horii, D.Y. Loh, and K. Nakayama. 1996. Mice lacking p27^{Kip1} display increased body size, multiple organ hyperplasia, retinal dysplasia, and pituitary tumor. *Cell* **85:** 707–720.

Norbury, C. and P. Nurse. 1992. Animal cell cycles and their control. *Annu. Rev. Biochem.* **61:** 441–470.

Nourse, J., E. Firpo, M.W. Flanagan, M. Meyerson, K. Polyak, M.-H. Lee, J. Massagué, G.R. Crabtree, and J.M. Roberts. 1994. Rapamycin prevents IL-2-mediated elimination of the cyclin-CDK kinase inhibitor, p27^{Kip1}. *Nature* **372:** 570–573.

Parker, S.B., G. Eichele, P. Zhang, A. Rawls, A.T. Sands, A. Bradley, E.N. Olson, J.W. Harper, and S.J. Elledge. 1995. p53-independent expression of p21^{Cip1} in muscle and other terminally differentiating cells. *Science* **267:** 1024–1027.

Polyak, K., M.-H. Lee, H. Erdjument-Bromage, A. Koff, P. Tempst, J.M. Roberts, and J. Massagué. 1994. Cloning of p27^{Kip1} a cyclin-cdk inhibitor and a potential mediator of extracellular antimitogenic signals. *Cell* **78:** 59–66.

Reynisdóttir, I. and J. Massagué. 1997. The subcellular locations of p15^{Ink4b} and p27^{Kip1} coordinate their inhibitory interactions with cdk4 and cdk2. *Genes & Dev.* **11:** 492–503.

Reynisdóttir, I., K. Polyak, A. Iavarone, and J. Massagué. 1995. Kip/Cip and Ink4 Cdk inhibitors cooperate to induce cell cycle arrest in response to TGF-β. *Genes & Dev.* **9:** 1831–1845.

Russo, A.A., P.D. Jeffrey, A. Patten, J. Massagué, and N. Pavletich. 1996. Crystal structure of the p27^{Kip1} cyclin-dependent kinase inhibitor bound to the cyclin A-cdk2 complex. *Nature* **382:** 325–331.

Scrable, H., W. Cavenee, F. Ghavimi, M. Lowell, K. Morgan, and C. Sapienza. 1989. A model for embryonal rhabdomyosarcoma tumorigenesis that involves genome imprinting. *Proc. Natl. Acad. Sci.* **86:** 7480–7484.

Serrano, M., H.-W. Lee, L. Chin, C. Cordon-Cardo, D. Beach, and R.A. DePinho. 1996. Role of the INK4a locus in tumor suppression. *Cell* **85:** 27–37.

Sherr, C.J. and J.M. Roberts. 1995. Inhibitors of mammalian G1 cyclin-dependent kinases. *Genes & Dev.* **9:** 1149–1163.

Slingerland, J.M., L. Hengst, C. Pan, D. Alexander, M. Stampfer, and S.I. Reed. 1994. A novel inhibitor of cyclin-cdk activity detected in transforming growth factor β-arrested epithelial cells. *Mol. Cell. Biol.* **14:** 3683–3694.

Steinman, R.A., B. Hoffman, A. Iro, C. Guillouf, D.A. Liebermann, and M.E. El-Houseini. 1994. Induction of p21 (WAF-1/CIP1) during differentiation. *Oncogene* **9:** 3389–3396.

Thompson, J.S., K.J. Reese, M.R. DeBaum, E.J. Perlman, and A.P. Feinberg. 1996. Reduced expression of the cyclin-dependent kinase inhibitor gene p57^{Kip2} in Wilms' tumor. *Cancer Res.* **56:** 5723–5727.

Tokino, T., T. Urano, T. Furuhata, M. Matsushima, T. Miyatsu, S. Sasaki, and Y. Nakamura. 1996. Characterization of the human p57^{Kip2} gene: Alternative splicing, insertion/deletion polymorphisms in VNTR sequences in the coding region, and mutational analysis. *Hum. Genet.* **97:** 625–631.

Toyoshima, H. and T. Hunter. 1994. p27, a novel inhibitor of G1 cyclin-Cdk protein kinase activity, is related to p21. *Cell* **78:** 67–74.

Tybulewicz, V.L.J., C.E. Crawford, P.K. Jackson, R.T. Bronson, and R.C. Mulligan. 1991. Neonatal lethality and lymphopenia in mice with a homozygous disruption of the c-able proto-oncogene. *Cell* **65:** 1153–1163.

Weinberg, R.A. 1995. The retinoblastoma protein and cell cycle control. *Cell* **81:** 323–330.

Wiedemann, H.R. 1983. Tumours and hemihypertrophy associated with Wiedemann-Beckwith syndrome. *Eur. J. Pediatr.* **141:** 129.

Downloaded from genesdev.cshlp.org on April 30, 2024 - Published by Cold Spring Harbor Laboratory Press

Ablation of the CDK inhibitor p57Kip2 results in increased apoptosis and delayed differentiation during mouse development.

Y Yan, J Frisén, M H Lee, et al.

Genes Dev. 1997, **11:**
Access the most recent version at doi:10.1101/gad.11.8.973

References This article cites 52 articles, 18 of which can be accessed free at:
http://genesdev.cshlp.org/content/11/8/973.full.html#ref-list-1

License

Email Alerting Service Receive free email alerts when new articles cite this article - sign up in the box at the top right corner of the article or **click here.**

Copyright © Cold Spring Harbor Laboratory Press